Asian Journal of Chemistry; Vol. 25, No. 13 (2013), 7539-7542

ASIAN JOURNAL OF CHEMISTRY

http://dx.doi.org/10.14233/ajchem.2013.15092

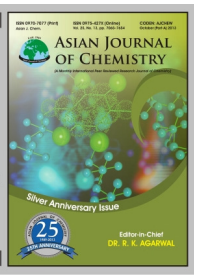

Synthesis of Fluorine Doped Zinc Oxide Particles by Hydrothermal Method

S. KERLI[1,*], U. ALVER[1,2], H. YAYKASLI[3], B. AVAR[4], A. TANRIVERDI[1] and C. KURSUN[3]

[1]Department of Physics, Kahramanmaras Sutcu Imam University, 46100 Kahramanmaras, Turkey
[2]Department of Electrical and Electronics Engineering, International University of Sarajevo, 71210 Sarajevo, Bosnia and Herzegovina
[3]Research and Development Center for University-Industry and Public Relations (USKIM), 46100 Kahramanmaras, Turkey
[4]SNTG Lab., Physics Engineering Department, Hacettepe University, Beytepe, 06800 Ankara, Turkey

*Corresponding author: Fax: +90 344 2191042; Tel: +90 344 2191487; E-mail: suleymankerli@yahoo.com

(*Received*: 4 January 2013; *Accepted*: 1 July 2013) AJC-13746

Fluorine doped ZnO particles were prepared by a simple hydrothermal technique in an autoclave at 200 ºC for 4 h. Obtained particles were annealed at 600 ºC and their physical properties were investigated. X-Ray diffraction measurements reveal that ZnO:F particles contain a wurtzite and simonkolleite structure. Thermal gravimetric measurements show that thermal decomposition of simonkolleite occurs at above 600 ºC. SEM images of particles show that the morphologies change from a flower-like structure to a rose-like structure with increasing fluorine concentration. Optical measurements revealed that absorbance edge values of fluorine doped ZnO particles are blue shifted.

Key Words: Fluorine doping, ZnO particles, Hydrothermal method, Zinc chloride.

INTRODUCTION

Zinc oxide with a wide band gap energy (3.37 eV) and a hexagonal wurtzite crystal structure has attracted a great deal of attention for its potential application including piezoelectric devices, transistors, photodiodes, photo catalysis, biomedicine, *etc*.[1-4]. Various synthesis methods such as wet-chemical route[5], chemical vapour deposition (CVD)[6], vapour-liquid-solid (VLS)[7], chemical solution methods[8] and hydrothermal method[9] have been used to grow doped ZnO micro/nano-crystals. Among these methods, the hydrothermal method is promising for fabricating ideal material with special morphology because of the simple, fast, less expensive, low growth temperature, high yield and scalable process. In recent years, introducing cationic impurities in ZnO structure offers an effective approach to adjust structural, optical and electrical properties[10-14]. An alternative way to adjust the physical properties of the ZnO particles is the replacement of oxygen ions (O^{2-}) in the ZnO lattice by anionic impurities, such as fluorine (F^{-})[15]. Most of the previous research works have focused on fluorine-doped ZnO thin films. There are less studies with fluorine doped ZnO particles. In addition, in many studies ZnO particles were synthesized by using zinc acetate or zinc nitrate precursor, but using zinc chloride as a precursor material is very seldom reported. In this paper, we have studied the fluorine doped ZnO particles (ZnO:F) prepared by hydrothermal technique using zinc chloride precursor and we have also investigated the effect of annealing on the thermal, structural, optical and morphological properties of ZnO:F particles.

EXPERIMENTAL

The precursor solution was prepared by dissolving 0.1 M of zinc chloride ($ZnCl_2$), 0.1 M of hexamethylenetetramine (HMT, $C_6H_{12}N_4$) and 0.1 M of ammonium fluoride (NH_4F) in 100 mL deionized water. The fluorine concentrations in precursor solutions were adjusted in terms of atomic percentage (0, 1, 3 and 5 at %) with respect to zinc. Hydrothermal growth was carried out at 200 ºC in an autoclave placed on a furnace for 4 h. After cooling naturally to room temperature, the transparent supernatant was removed by pipette and white ZnO precipitates were left. The obtained particles were washed with distilled water several times and dried at room temperature in air for further characterization. All experimental conditions were kept the same for all samples. To investigate the effect of annealing, the particles were annealed at 600 ºC for 1 h in air. The crystal structures of ZnO particles were investigated by Philips X'Pert Pro X-ray diffractometer (XRD), with CuK_α radiation, the surface morphologies were observed using a Zeiss EVO-LS10 scanning electron microscopy (SEM). Thermal gravimetric and differential thermal analysis (TG-DTA) curves were conducted with a Perkin-Elmer Diamond TG-DTA at a heating rate of 40 ºC/min in air. Optical properties of samples were obtained by using a Shimadzu UV-1800 ultraviolet-visible spectrometer (UV-VIS).

RESULTS AND DISCUSSION

XRD patterns of unannealed and annealed ZnO:F particles are shown in Fig. 1a-b. Fig. 1a shows XRD patterns of ZnO:F particles prepared in various fluorine concentration. As seen in Fig. 1a, diffraction peaks indicate that undoped ZnO particles have a hexagonal wurtzite structure (PDF-2, reference code: 01-079-2205). For the fluorine doped ZnO particles, in addition to peaks belonging to pure ZnO structure, some other low intensity impurity peaks have been observed at 2θ values especially between 30 and 35º. Moreover, the intensities of these impurity peaks increase with increasing fluorine addition, while the intensities of ZnO peaks are decreasing. When the fluorine concentration reaches to 5 at %, a new diffraction pattern ascribed to zinc chloride hydroxide monohydrate (simonkolleite), $Zn_5(OH)_8Cl_2H_2O$ in accordance with the PDF-2, reference code: 01-076-0922 is occurred. A detail analyses show that the impurity peaks shown in 1 and 3 at % fluorine doped ZnO particles arises from simonkolleite structure. The reason for the formation of this simonkolleite structure might be decrease the zinc ion concentration in precursor solution while the fluorine concentration is increasing. XRD pattern of the annealed ZnO nanoparticles at 600 ºC for 1 h is shown in Fig. 1b. The absence of simonkolleite structure in the XRD data demonstrates the complete removal of impurities from ZnO:F nanoparticle samples after annealing. In addition, as shown in Fig. 1b, the peak intensities of the planes are found to decrease with increasing fluorine doping concentration for all samples. This indicates that the crystalline quality of the ZnO:F particles degrades when the fluorine doping increases.

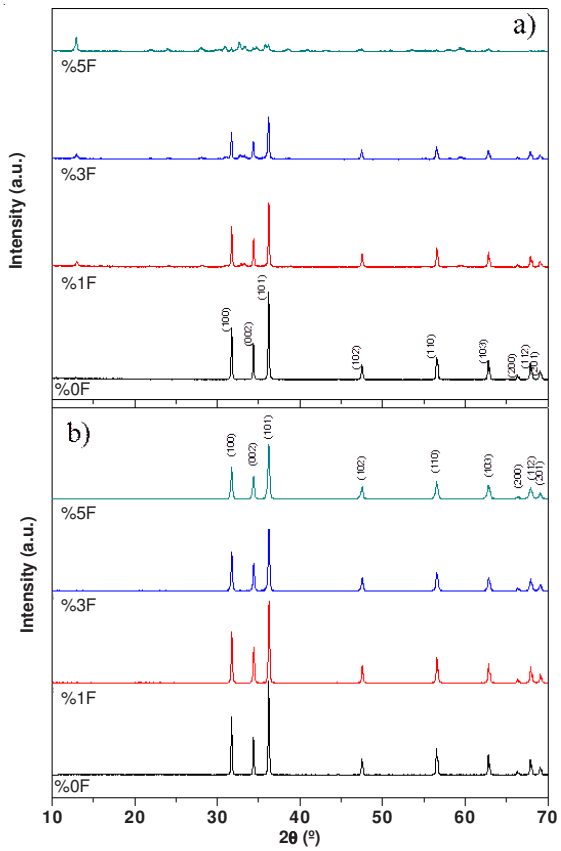

Fig. 1. (a) XRD patterns of (a) fluorine doped (b) annealed fluorine doped ZnO particles

TG-DTA curves of ZnO and 5 at. % fluorine doped ZnO particles are shown Fig. 2a-b. In Fig. 2a, the TGA curves show two step weight losses. The first step at around 100-300 ºC corresponds to the loss of water molecules on the surface and interlayer of the ZnO particles. The second step occurs at 300-600 ºC due to the decomposition of hydroxide and other compounds in the precursor solutions. As seen Fig. 2a, the total weight loss is about 11 % for the ZnO particles. For the simonkolleite structure, the first weight loss occurred at a temperature of between 100 and 300 ºC, which corresponded to the loss of water molecules from $Zn_5(OH)_8C_{l2}H_2O$, to form ZnO and zinc chloride and hydrochloric acid.

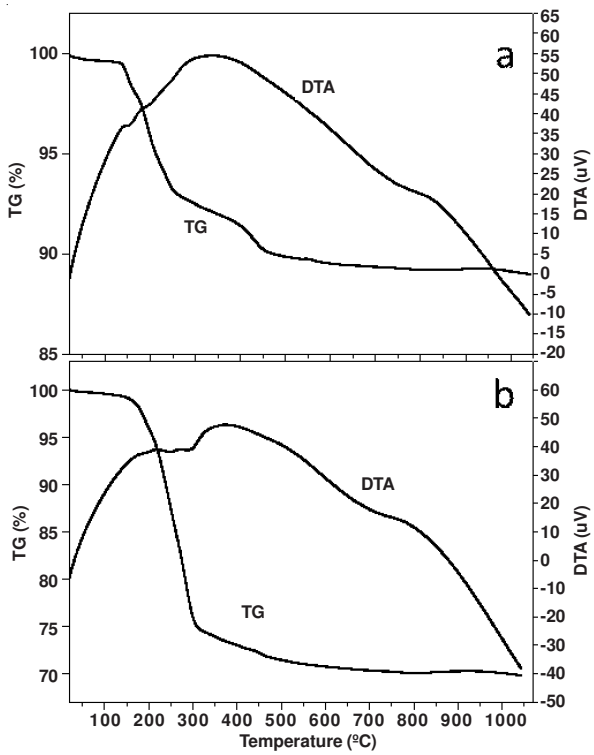

Fig. 2. TG-DTA trace for (a) ZnO particles (b) 5 % fluorine doped ZnO

The second weight loss occurred at in between 300 and 600 ºC, which was attributed to the conversion of $Zn_5(OH)_8Cl_2{\cdot}H_2O$ to complete zinc oxide. From Fig. 2b, the weight loss of simonkolleite structure is measured about 28 % which is close to theoretical value (26.3 %). We could not observe any strong DTA peak corresponding to phase transition in Fig. 2a-b. This might be high heating rate (40 ºC/min). The results of thermal analysis indicate that the samples contain some hydroxyl group and impurities. The XRD results (Fig. 1a) confirmed this idea, because some low intensity peaks other than wurtzite ZnO were observed in XRD analysis for unannealed samples. As seen in Fig. 2a-b, the completion temperature of thermal-decomposing is about 600 ºC and thus it was chosen as the calcination temperature to prepare ZnO:F structures.

SEM images of prepared fluorine doped ZnO particles shown in Fig. 3a-d. As seen in these figures, the distribution, size and microstructure of the ZnO powders change with the fluorine doping concentration significantly for all samples. As seen in Fig. 3a, undoped ZnO particles show a flower-like

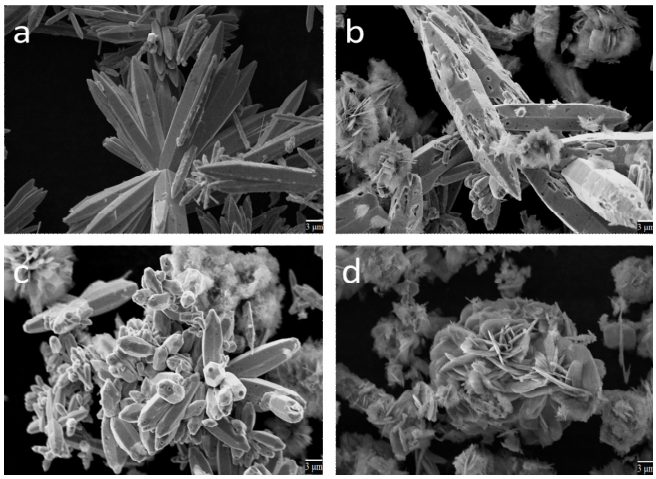

Fig. 3. SEM images of (a) ZnO, (b) 1 at %, (c) 3 at %, (d) 5 at % fluorine doped ZnO particles

structure consisting of many sharp-tipped ZnO rods which originated from a single center. In Fig. 3b with the fluorine adding, some rose-like structures associated with simonkolleite structure start to appear in SEM image. When the fluorine concentration was 5 at %, the flower like structure was completely transformed to rose-like structure (Fig. 3d). These results are in agreement with the XRD result, as shown in Fig. 1a. The annealed fluorine doped ZnO particles are presented in Fig. 4a-d. As seen annealed images, rose-like structure assigned to simonkolleite disappears and the lengths of rod particles are decreasing with increasing fluorine concentration in structure.

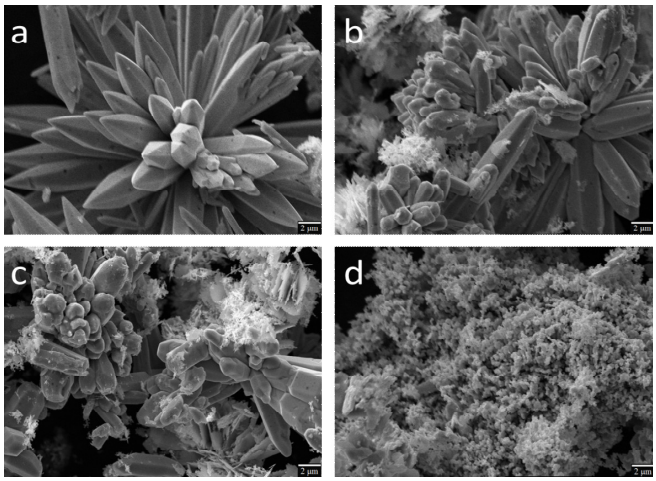

Fig. 4. SEM images of annealed (a) ZnO, (b) 1 at %, (c) 3 at %, (d) 5 at % fluorine doped ZnO particles

The optical properties of unannealed and annealed fluorine doped ZnO particles were investigated by using UV-visible absorbance spectra (Fig. 5a-b). All absorption curves exhibit an observable absorption in the range 320-400 nm, with the absorption edge in between 370 and 380 nm, due to the large exciton binding energy. Insets of Fig. 5a-b show absorbance edge shift of fluorine doped ZnO particles. It can be seen that the absorbance edge decreases with increasing fluorine concentration for all samples. The movement of absorbance edge to the shorter wavelength (higher band gap) is the Burnstein-Moss effect[16], which is due to the increase

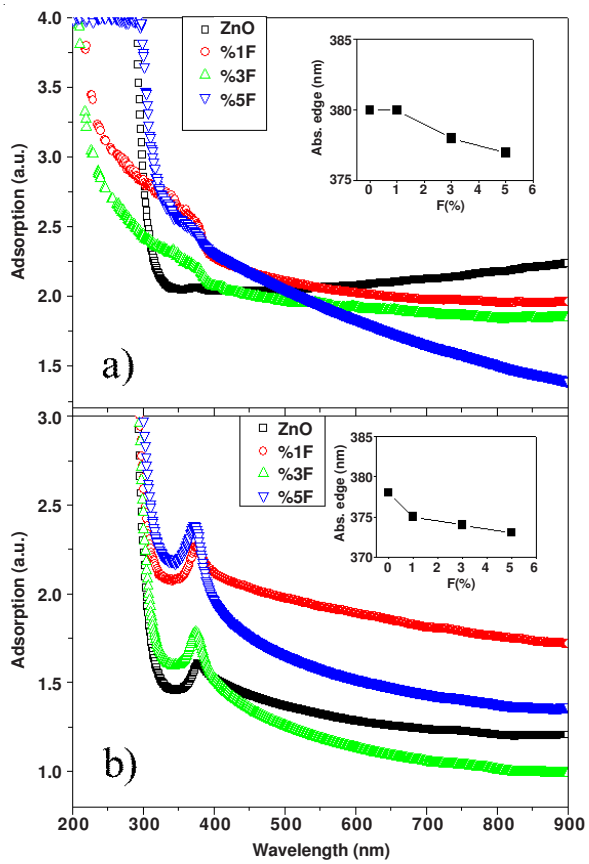

Fig. 5. Absorption spectra of (a) unannealed and (b) annealed fluorine doped ZnO particles. Insets show the change in absorption edge with fluorine concentration

of carrier concentration. As seen in Fig. 5b, after annealing the absorption peaks are observed much sharper and clear and the absorbance edge decreases with increasing fluorine concentration for all samples. These obtained results are in agreement with the work done by Gonzalez *et al.*[8], they reported that the band gap energy is increased with the 5 at % fluorine doping.

Conclusion

The present investigation showed an influence of fluorine on the formation of ZnO particles, synthesized by hydrothermal method. XRD, SEM and TGA measurements show that obtained particles have a simonkolleite structure as well as wurtzite structure. The XRD patterns show that the wurtzite structure turns into simonkolleite structure when the doping concentration reaches to 5 at %. Thermal gravimetric measurements show that thermal decomposition of simonkolleite is occurred at 600 ºC and above. The morphologies of ZnO particles are influenced by addition of fluorine impurity. The shapes of fluorine doped ZnO particles are altered from a flower-like to a rose-like with increasing fluorine concentration. From UV-VIS spectrum, we find that absorption edges of ZnO powders are decreasing with increasing fluorine concentration.

REFERENCES

1. Y.C. Kong, D.P. Yu, B. Zhang, W. Fang and S.Q. Feng, *Appl. Phys. Lett.*, **78**, 407 (2001).
2. Y.W. Zhu, H.Z. Zhang, X.C. Sun, S.Q. Feng, J. Xu, Q. Zhao, B. Xiang and R.M. Wang, *Appl. Phys. Lett.*, **83**, 144 (2003).
3. D.A. Lamb and S.J.C. Irvine, *J. Cryst. Growth*, **273**, 111 (2004).

4. L.A. Alkhtaby, S. Husain1, W. Khan and S.A.H. Naqvi, *Asian J. Chem.*, **23**, 5607 (2011).
5. C.-H. Ku, H.-H. Yang, G.-R. Chen and J.-J. Wu, *Cryst. Growth Des*., **8**, 283 (2008).
6. C.L. Wu, Li Chang, H.G. Chen, C.W. Lin, T.F. Chang, Y.C. Chao and J.K. Yan, *Thin Solid Films*, **498**, 137 (2006).
7. H. Huang, Y. Wu, H. Feick, N. Tran, E. Weber and P. Yang, *Adv. Mater*., **13**, 113 (2001).
8. R. Gonzalez-Hernandez, A.I. Martinez, C. Falcony, A.A Lopez, M.I. Pech-Canul and H.M. Hdz-Garcia, *Mater. Lett*., **64**, 1493 (2010).
9. R.R. Mohan, K. Rajendran, K. Sambath and O.M. Saravanakumar, *Asian J. Chem.*, **25**, S107 (2013).
10. E. Bacaksiz, S. Aksu, S. Yilmaz, M. Parlak and M. Altunbas, *Thin Solid Films*, **518**, 4076 (2010).
11. S. Huang, Q. Xiao, H. Zhou, D. Wang and W. Jiang, *J. Alloy Comp*., **486**, L24 (2009).
12. Y.S. Wang, P.J. Thomas and P. O'Brien, *J. Phys. Chem. B*, **110**, 21412 (2006).
13. B.J. Lokhande, P.S. Patil and M.D. Uplane, *Physica B*, **302-303**, 59 (2001).
14. T. Al-Harbi, *J. Alloy Comp*., **509**, 387 (2011).
15. A. Sanchez-Juarez, A. Tiburcio-Silver and A. Ortiz, *Sol. Energy Mater. Sol. Cells*, **52**, 301 (1998).
16. E. Burnstein, *Phys. Rev*., **93**, 632 (1954).